Article

DNA Modified Fe3O4@Au Magnetic Nanoparticles as Selective Probes for Simultaneous Detection of Heavy Metal Ions

Peng Miao, Yuguo Tang, and Lei Wang

ACS Appl. Mater. Interfaces, **Just Accepted Manuscript** • DOI: 10.1021/acsami.6b14247 • Publication Date (Web): 12 Jan 2017

DNA Modified Fe_3O_4@Au Magnetic Nanoparticles as Selective Probes for Simultaneous Detection of Heavy Metal Ions

Peng Miao,[*,†,‡] *Yuguo Tang,*[†,‡] *and Lei Wang*[†]

[†]Suzhou Institute of Biomedical Engineering and Technology, Chinese Academy of Sciences, Suzhou 215163, People's Republic of China

[‡]University of Chinese Academy of Sciences, Beijing 100049, People's Republic of China

ABSTRACT: Driven by the urgent need to detect trace heavy metal ions in various real water samples, this article demonstrates for the first time an electrochemical biosensor based on DNA modified Fe_3O_4@Au magnetic nanoparticles (NPs). Three DNA probes are designed to contain certain mismatched base pairs. One is thiolated and modified on the surface of Fe_3O_4@Au NPs (DNA 1). The other two probes (DNA 2 and 3) are labeled with two independent electrochemical species. Stable structures of cytosine-Ag^+-cytosine and thymine-Hg^{2+}-thymine formed in the presence of Ag^+ and Hg^{2+} can assist the hybridization of DNA 1/DNA 2 and DNA 1/DNA 3, which locate corresponding electrochemical species onto the surface of the magnetic NPs. The achieved nanocomposites are then used as selective electrochemical probes for the detection of heavy metal ions by recording the square wave voltammetry signals. Simultaneous detection of Ag^+ and Hg^{2+} is demonstrated without significant interference and their individual high sensitivities are fundamentally preserved, which meet the requirements of U.S. Environmental Protection Agency (USEPA). Furthermore, the proposed method has been challenged by various real water samples. The results confirm the DNA modified magnetic NPs based sensing method may have potential applications for the monitoring of heavy metal ions in real sample analysis.

KEYWORDS: magnetic nanoparticles, Ag^+, Hg^{2+}, DNA mismatch, electrochemical detection

INTRODUCTION

Hazardous heavy metal ions from geochemical cycling and industrial pollution cause pervasive environmental pressure, which has been an important concern throughout the world for decades.[1] The ions like silver ion (Ag^{+}) and mercury ion (Hg^{2+}) may exist in a variety of sources (e.g., surface water, drinking water, industrial waste and food), which are non-naturally degradable. These exposed ions have strong biological enrichment and can lead to a series of disorders of human body mechanisms. For instance, accumulation of low concentration of Hg^{2+} in human body may cause sensory disturbances, kidney failure, and cardiovascular system destruction.[2-3] The toxicity of silver mainly originates from the ability of Ag^{+} to bind with various metabolites and inactivate sulfhydryl enzymes. After accumulated in human body, Ag^{+} is able to trigger severe damages of cell membrane via extracellular mechanisms and induce skin irritation, stomach distress, organ edema, and even death.[4-5]

Currently, people are easily exposed to these heavy metal ions when some human activities are exerted improperly. For example, alkali processing, incineration of coal and metal mining may result in persistent contaminants. Therefore, pollution caused by heavy metal ions, especially by Ag^{+} and Hg^{2+}, is regarded as a necessary aspect of environmental monitoring. Both of World Health Organization (WHO) and U.S. Environmental Protection Agency (USEPA) have set rigid limits on the range of permissible levels.[6-8] It has been reported that tracing heavy metal ions at nM levels are of great importance.[9-10] In recent decades, numerous analytical strategies have been conventionally employed and well established including atomic absorption spectrometry (AAS),[11] inductively coupled plasma-mass spectrometry (ICP-MS),[12] and inductively coupled plasma optical emission spectrometry (ICP-OES).[13] Although the reliability of these methods are in no doubt, precision instruments with high cost or tedious sample

preparation processes are always required. More significantly, these analytical systems lack portability and cannot meet the demands for field-based or on-site water monitoring by personnel with limited training. Nowadays, a diversity of novel schemes have been developed for the detection of heavy metal ions, e.g., colorimetric assay,[14-15] electrochemical sensor,[16-17] surface enhanced Raman scattering (SERS) spectroscopy[18-19] and fluorescence spectroscopy.[20-21] Nanomaterials are always used to improve the analytical performances for heavy metal ions assays including carbon nanotubes,[22] gold nanoparticles (Au NPs),[23] and polymer NPs.[24] For example, Darbha et al. explored nonlinear optical properties of modified Au NPs and recorded hyper Rayleigh scattering intensities for rapid, easy and reliable screening of Hg^{2+}.[25] Yang et al. designed a fluorescent nanoprobe coupling rhodamine B isothiocyanate and MoS_2 nanosheets to realize sensitive detection of Ag^{+}.[26] Lu et al. functionalized graphene oxide with oligonucleotide and employed DNase I assisted target recycling amplification for Hg^{2+} detection.[27]

Since Ag^{+} and Hg^{2+} are usually coexisting in different samples like surface water, soil and some biological systems,[28] the development of sensing methods to simultaneously detect these heavy metal ions are imperative to replace the combination of different sensors for the detection of only one target. Multiplex analysis method could not only avoid the inconvenience of using different techniques or experimental conditions, but also economize cost, time and complexity. However, only a few relevant simultaneous detection methods have been reported. Liu and Lin developed a paper-based colorimetric array test strip for multi-ion analysis using specifically responsive indicators in typical matrixes.[29] Zuo et al. employed WS_2 nanosheet as fluorescence quenching reagent for dual-color detection of Ag^{+} and Hg^{2+}.[30] Zeng et al. fabricated a polyadenine-DNA-mediated approach for an alkyne-coded surface enhanced Raman scattering (SERS) test kit, which could realize rapid analysis of two target ions.[31] Nevertheless, it is

difficult to achieve both high sensitivity and convenient sensing strategy for stable practical applications. To date, simultaneous detection of Ag^+ and Hg^{2+} for practical use still remains a challenge.

Electrochemical techniques have the advantages of low cost, easy operation, fast response, high sensitivity and specificity, which are suitable for ion sensing.[32-34] Herein, an electrochemical sensing strategy is proposed for highly sensitive and selective detection of Ag^+ and Hg^{2+} employing DNA modified Fe_3O_4@Au NPs and magnetic glassy carbon electrode (MGCE). DNA probes labeled with two electrochemical species, ferrocene (Fc) and methylene blue (MB), can be used to represent the levels of different types of heavy metal ions simultaneously. Magnetic nanomaterials have been intensively explored for various technological application.[35-36] Fe_3O_4 NPs are one of the most widely used magnetic nanomaterials, which has inherent high surface to volume ratio and magnetic property. They can be used as different forms including $MnFe_2O_4$ NPs, Fe_3O_4@Au NPs, Fe_3O_4@Pt NPs, and Fe_3O_4@carbon dots nanocomposites.[37-39] DNA modified Fe_3O_4@Au NPs and MGCE are used in this work, which eliminate complicated electrode modification process. Stable metal ion-coordinated DNA base pairs on the surface NPs are utilized for the recognition of targets. More concretely, cytosine-cytosine (C-C) and thymine-thymine (T-T) mismatches in DNA duplexes are designed to strongly bind to Ag^+ and Hg^{2+}, respectively. The proposed method is able to measure trace Ag^+ and Hg^{2+} with the concentrations lower than the toxicity levels in drinking water defined by USEPA (Ag^+: 460 nM; Hg^{2+}: 10 nM).

EXPERIMENTAL SECTION

Chemicals and Instruments. MGCE was purchased from Tianjin Incole Union Technology Co., Ltd. (Tianjin, China). Gold(III) chloride trihydrate ($HAuCl_4 \cdot 3H_2O$), tris(2-carboxyethyl)phosphine hydrochloride (TCEP), sodium borohydride ($NaBH_4$) and Iron(III) chloride hexahydrate ($FeCl_3 \cdot 6H_2O$) were purchased from Sigma (USA). Ethylene glycol and sodium acetate (NaAc) were purchased from Shanghai Aladdin Reagent Company (China). Mercury nitrate was ordered from Guangdong Longxi Chemical Plant (China). Silver nitrate was obtained from Nanjing Chemical Reagent Co., Ltd. (China). All other chemicals were of analytical grade and used as received. Oligonucleotides were synthesized and purified by Sangon Biotech Co., Ltd. (China). DNA 1 was thiolated with a $-(CH_2)_6-$ spacer at the 5' end. DNA 2 and DNA 3 were labeled with Fc and MB at the 5' end, respectively (Table S1). The underlined bases constitute C-C and T-T mismatched base pairs, respectively. Scanning electron microscopic (SEM) images were taken by using a Hitachi S4800 scanning electron microscopy (Hitachi, Japan). The crystalline phases were recorded by X-ray diffraction (XRD, Bruker Co. Ltd., Germany).

Synthesis of Pristine Fe_3O_4 and Fe_3O_4@Au NPs. Pristine Fe_3O_4 NPs were synthesized by means of a hydrothermal method.[40] Briefly, 1.35 g of $FeCl_3 \cdot 6H_2O$ was dissolved in 40 mL of ethylene glycol with constant mechanical stirring. After a clear solution was formed, 3.6 g of NaAc was added. The mixture was continually stirred for 0.5 h and the temperature was kept at 200 ºC for 9 h. After cooling to room temperature, a black precipitate was obtained, which was collected by a magnet. The prepared pristine Fe_3O_4 NPs were then washed with ethanol for three times to remove residual matrix. Then, the Fe_3O_4 NPs were dried under vacuum at 50 ºC.

The procedure to prepare Fe_3O_4@Au NPs was as follows. First, 15 mg of Fe_3O_4 NPs were dispersed in 150 mL of double-distilled water. Ultrasonication was then performed. Next, 3 mL

of $HAuCl_4$ aqueous solution with the concentration of 6 mg/mL was added to the above solution and the mixture was kept at 0 ºC with constant mechanical stirring for 1 h. Afterward, ice-cold $NaBH_4$ solution with the concentration of 0.2 M was prepared and 0.9 mL of the solution was slowly added to the mixture of Fe_3O_4 NPs and $HAuCl_4$ (within 4 min). The reaction was under stirring at 0 ºC for 15 min. Solution color changed from light brown to dark purple. The prepared Fe_3O_4@Au NPs were collected by a magnet and washed with ethanol for three times. Finally, the products were dried under vacuum at 50 ºC.

Preparation of DNA Modified Fe_3O_4@Au NPs. Pristine Fe_3O_4@Au NPs were dispersed in double-distilled water with the concentration of 1 mg/mL. DNA 1 probe was prepared in the buffer (10 mM Tris–HCl, 1 mM EDTA, 10 mM TCEP, and 0.1M NaCl). Next, the Fe_3O_4@Au NPs colloid was blended with DNA 1 probe with the final concentration of 5 μM. The mixture was left undisturbed for 16 h and then "aged" in salts (10 mM phosphate, 0.1 M KNO_3, pH 7.0) for 24 h to make DNA 1 probes ordered and vertical. To remove excess reagents, DNA modified Fe_3O_4@Au NPs were separated by a magnet and washed by 10 mM phosphate buffer (pH 7.4) containing 0.25 M NaCl.

Electrode Cleaning. GCE was cleaned before further use. Briefly, it was soaked in piranha solution (98% H_2SO_4 : 30% H_2O_2 = 3 : 1) for about 5 min so as to remove any adsorbed materials (Caution: Piranha solution dangerously attacks organic matter!). After carefully rinsed with double-distilled water, the GCE was polished with P3000 silicon carbide paper to a mirror-like surface. Next, the electrode was sonicated in ethanol for 5 min and then in water for another 5 min. Subsequently, it was dried with nitrogen and was ready for further use.

Detection of Ag^+ and Hg^{2+}. Standard Ag^+ and Hg^{2+} solutions with a series of concentrations were prepared in pure water (10, 20, 50, 80, 100, 150, 200, 400 nM). The solutions were blended with DNA 1 modified Fe_3O_4@Au NPs (1 mg/mL), DNA 2 (3 μM) and DNA 3 (3 μM) at room temperature for 1 h. Subsequently, MGCEs were immersed in these mixtures for 2 min. After rinsed with water, MGCEs were electrochemically measured.

Electrochemical Measurement. Electrochemical measurements were carried out on a model CHI660D Electrochemical Analyzer (CH Instruments) with a conventional three-electrode system, in which a saturated calomel electrode (SCE) was used as the reference electrode, a platinum wire electrode as the counter electrode and a MGCE (3 mm in diameter) as the working electrode (Figure S1). All electrolytes were thoroughly deoxygenated by bubbling nitrogen through the solutions before electrochemical measurements. Electrochemical impedance spectroscopy (EIS) was performed in 5 mM $[Fe(CN)_6]^{3-/4-}$ with 1 M KCl to investigate the interfacial properties at the MGCE during different modification stages. The biasing potential was 0.189 V, amplitude was 5 mV and the frequency range was 0.1 Hz to 100 k Hz. Square wave voltammetry (SWV) was performed in 20 mM Tris-HCl (pH 7.4) containing 140 mM NaCl and 5 mM $MgCl_2$ to probe the electrochemistry of Fc and MB.[41] Modulation amplitude was 25 mV, frequency was 60 Hz and the step potential was 4 mV.

RESULTS AND DISCUSSION

Sensing Principle. In this work, we have prepared DNA modified Fe_3O_4@Au NPs, which are employed in an electrochemical system for the detection of heavy metal ions. Selective recognition of Ag^+ and Hg^{2+} are based on the generation of metal-mediated base pairs in DNA

duplexes using C-C and T-T mismatches respectively.[42-43] Detailed sensing principle is illustrated in Scheme 1. Generally, Fe_3O_4@Au NPs are formed by the borohydride reduction of $HAuCl_4$ on the surface of Fe_3O_4 NPs. Thiolated DNA 1 probe is able to be linked onto the NPs via gold-sulfur chemistry. The other two DNA probes labeled with Fc and MB are designed to contain mismatched sites with DNA 1 probe, and the hybridization events occur on the basis of C-Ag^+-C and T-Hg^{2+}-T coordination chemistry. Owning to the magnetic property of the electrode, the modified Fe_3O_4@Au NPs can be easily immobilized on the electrode surface (Figure S2). Fe_3O_4@Au NPs with the concentration up to 10 mg/mL can be isolated from the solution in 2 min, making the solution transparent. Afterward, the electrochemical species can be detected by SWV to represent corresponding target heavy metal ions.

This proposed method exhibit many advantages compared with other assay methods. First, Ag^+ and Hg^{2+} assisted hybridization events occur in liquid, which are much faster than those in solid-liquid interface. Second, Fe_3O_4@Au NPs possess enormously large surface area than a flat solid phase for molecule immobilization and reaction. Third, benefited from the magnetic property, electrochemical species are easily brought to the magnetic electrode for direct electrochemical measurement, which eliminates tedious electrode modification procedure and accelerate the analysis rate. The interference from sample matrix can also be significantly minimized. Fourth, Fc and MB with discreted current peaks are designed to represent two targets, which promises simultaneous detection of Ag^+ and Hg^{2+}. Fifth, the assay method does not require any sophisticated instrumentations or amplification processes, which is well suitable for potential practical applications. Sixth, the developed biosensor has potential to be further developed as a universal platform for the detection of other heavy metal ions in the future. For

example, current recognition elements (mismatched base pairs) could be replaced as DNAzymes for the detection of Pb^{2+} and Cu^{2+}.[44]

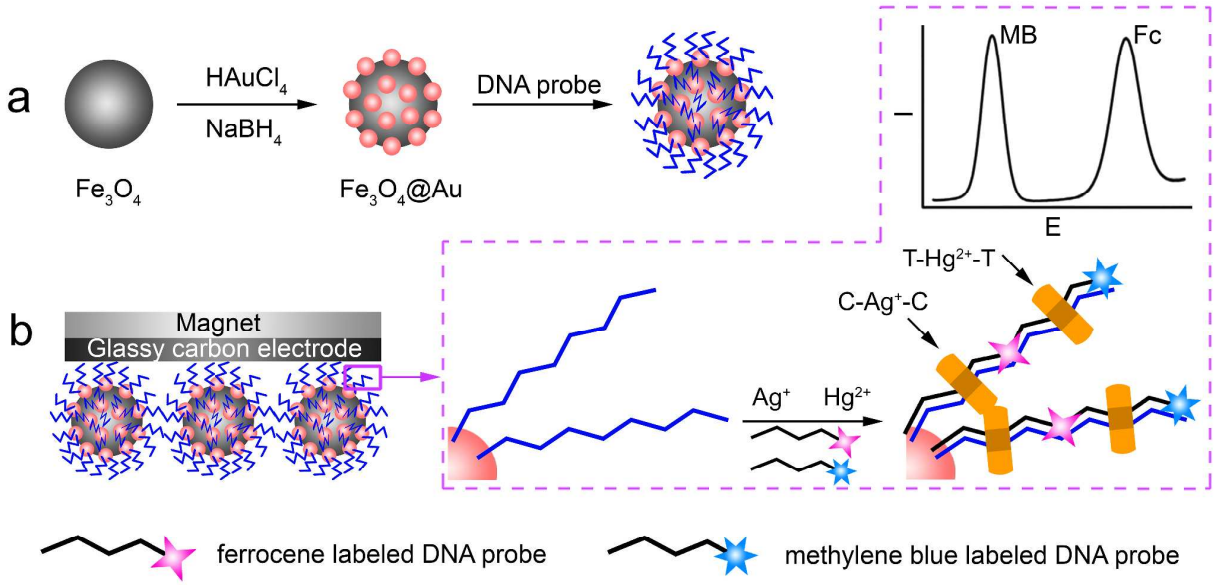

Scheme 1. (a) The preparation schematic diagram of DNA modified Fe_3O_4@Au NPs. (b) Schematic diagram of the procedure used for simultaneous detection of Ag^+ and Hg^{2+}.

Characterization of the Magnetic NPs. The morphologies and structures of the prepared Fe_3O_4 NPs and Fe_3O_4@Au NPs are investigated by SEM. From Figure 1a we can see that the as-prepared Fe_3O_4 NPs are uniform spherical particles with the mean diameter about 150 nm. As shown in Figure 1b, the Fe_3O_4 NPs are coated with many bright NPs, which are attributed to Au NPs.

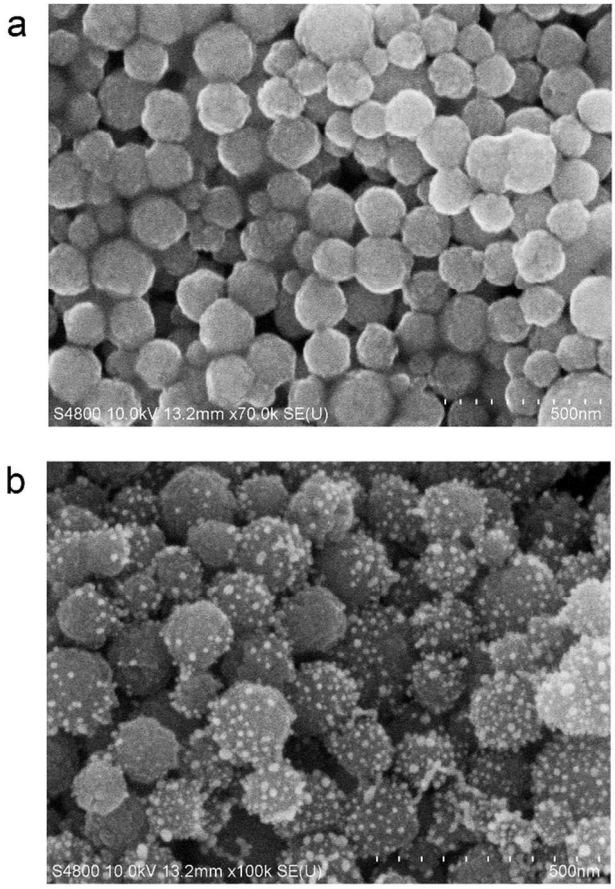

Figure 1. SEM images of (a) Fe_3O_4 NPs and (b) Fe_3O_4@Au NPs.

To further confirm the successful synthesis of Fe_3O_4@Au NPs, we have then studied XRD patterns of the prepared nanomaterials (Figure 2a). In the curve for Fe_3O_4 NPs, eight peaks are observed (30.3°, 35.6°, 43.4°, 53.7°, 57.2°, 62.8°, 67.9° and 73.8°), which correspond to the (220), (311), (400), (422), (511), (440), (442) and (533) diffraction peaks of inverse spinel structure (JCPDS no. 19-0629). In the curve for Fe_3O_4@Au NPs, four more peaks at 38.4°, 44.6°, 64.9° and 77.8° are observed, which are indexed as the (111), (200), (220) and (311) diffraction peaks of Au crystal with a cubic phase (JCPDS no. 04-0784). As shown in Figure 2b, Fe_3O_4 NPs solution was brown in color and shows no absorption band in UV-vis spectrum. However,

Fe_3O_4@Au NPs is purple black in color and shows a typical absorption band around 550 nm, which may be attributed to the surface plasmon resonance of Au NPs.

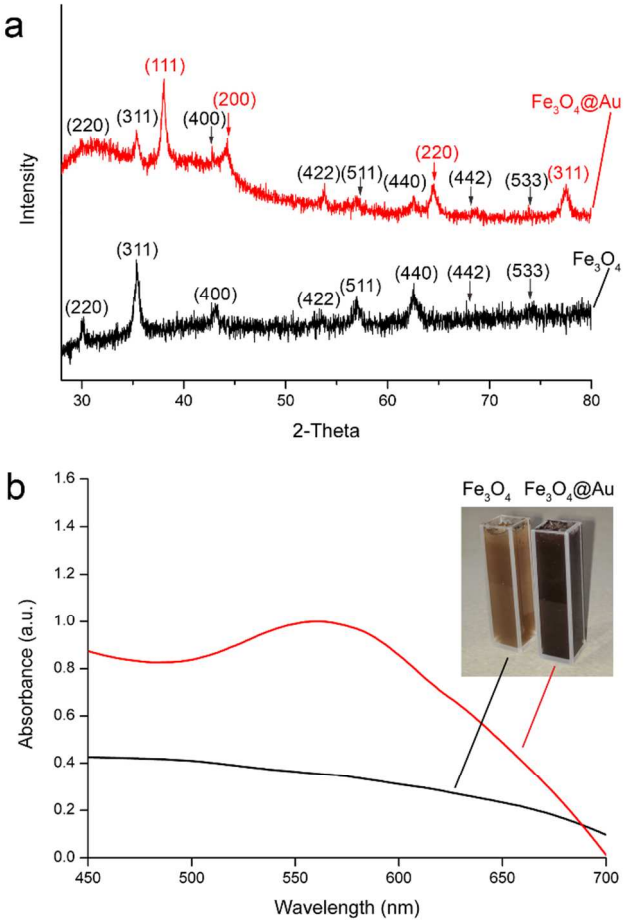

Figure 2. (a) XRD patterns and (b) UV-vis spectra of Fe_3O_4 NPs and Fe_3O_4@Au NPs with corresponding inset photographs.

We have then applied EIS to preliminarily demonstrate successful immobilization of DNA probes onto the Fe_3O_4@Au NPs. Nyquist diagrams are shown in Figure 3. Curve a stands for Fe_3O_4@Au NPs modified MGCE, which is a straight line, indicating excellent electron transfer

capability. After the modification of DNA 1, the phosphate backbone of DNA repels strongly the negatively charged redox probe $[Fe(CN)_6]^{3-/4-}$ and a large semicircle portion is observed which corresponds to the electron transfer controlled process. Due to the mismatches between DNA 1/DNA 2 and DNA 1/ DNA 3, hybridization events cannot occur efficiently. Therefore, after the immobilization of the mixture of Fe_3O_4@Au NPs-DNA 1, DNA 2 and DNA 3, the semicircle portion is not significantly changed (curve c). On the other hand, positively charged Ag^+ or Hg^{2+} (100 nM) could be adsorbed on Fe_3O_4@Au NPs-DNA 1, which reduces the semicircle portions (curve d and e). Moreover, the hybridization events assisted by Ag^+ or Hg^{2+} may locate more DNA probes on the magnetic NPs, which can be reflected by the much larger semicircle portions in the nyquist diagrams (curves f, g and h). The EIS experimental results thus confirm the feasibility of the sensing strategy.

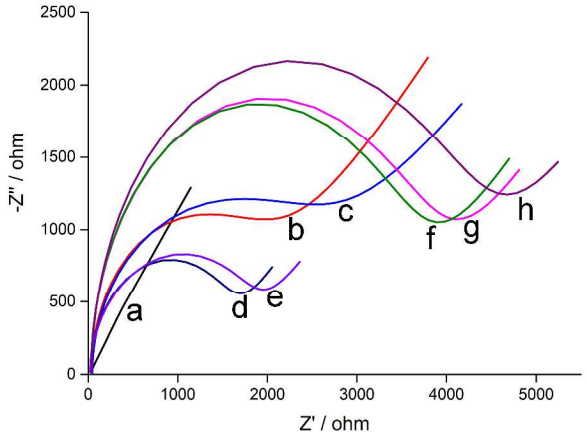

Figure 3. Nyquist diagrams of EIS for MGCE modified with (a) Fe_3O_4@Au NPs, (b) Fe_3O_4@Au NPs-DNA 1, (c) mixture of Fe_3O_4@Au NPs-DNA 1, DNA 2 and DNA 3, (d) mixture of Fe_3O_4@Au NPs-DNA 1 and Ag^+, (e) mixture of Fe_3O_4@Au NPs-DNA 1 and Hg^{2+}, (f) mixture of Fe_3O_4@Au NPs-DNA 1, Ag^+ and DNA 2, (g) mixture of Fe_3O_4@Au NPs-DNA 1, Hg^{2+} and DNA 3, (h) mixture of Fe_3O_4@Au NPs-DNA 1, Ag^+, Hg^{2+}, DNA2 and DNA 3.

Analysis of Ag^+ and Hg^{2+}. SWV are performed to probe the electrochemistry of the modified electrode. As shown in Figure 4, no current peaks are observed for bare MGCE, Fe_3O_4@Au NPs attached MGCE, Fe_3O_4@Au NPs-DNA 1 attached MGCE in the presence and absence of Ag^+ and Hg^{2+}, verifying zero background signal. Ag^+ and Hg^{2+} participate the formation of stable C-Ag^+-C and T-Hg^{2+}-T structures, which assist the hybridization events of DNA 1/DNA 2 and DNA 1/DNA 3 on the surface of DNA 1 modified Fe_3O_4@Au NPs, respectively. Thus, significant current peak (Fc) at 0.36 V appears in the presence of Ag^+ and current peak (MB) at -0.39 V emerges in the presence of Hg^{2+}. With the existence of both Ag^+ and Hg^{2+}, both of the two discreted current peaks can be observed, showing the potential to simultaneous detect Ag^+ and Hg^{2+}.

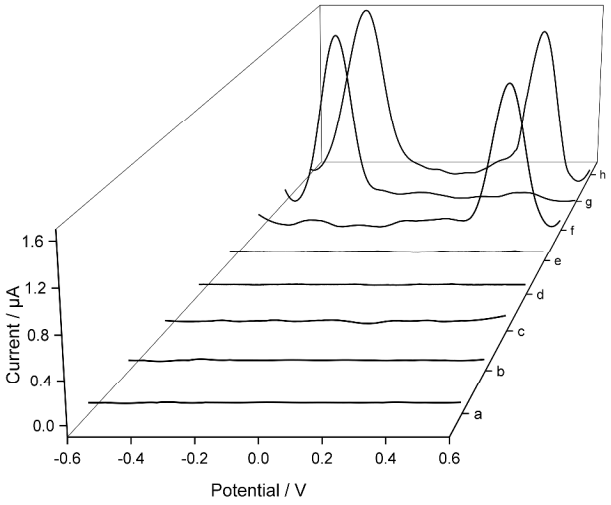

Figure 4. SWVs corresponding to (a) bare MGCE, (b) Fe_3O_4@Au NPs attached MGCE, (c) Fe_3O_4@Au NPs-DNA 1 attached MGCE, (d) after incubation with Ag^+ (100 nM), (e) after incubation with Hg^{2+} (100 nM), Fe_3O_4@Au NPs-DNA 1 attached MGCE after incubation with DNA 2, DNA 3 and (f) Ag^+ (100 nM), (g) Hg^{2+} (100 nM), (h) Ag^+ (100 nM) and Hg^{2+} (100 nM). The curves have been baseline corrected.

Before quantitative detection of target ions, the concentrations of DNA 1 and magnetic NPs are optimized (Figure S3). Larger amount of DNA 1 and magnetic NPs can link more electrochemical species in the presence of sufficient target heavy metal ions coupled with DNA 2 and DNA 3. Optimized concentrations are 5 μM for DNA 1 and 1 mg/mL for magnetic NPs respectively. Then, the sensitivity and dynamic range of this sensing strategy are monitored with Ag^+ and Hg^{2+} standards, separately. As shown in Figure 5, SWV peak of Fc displays a dependence upon Ag^+ concentration. More Ag^+ locate more Fc on the surface of the magnetic NPs, which are absorbed on the electrode interface for electrochemical measurement. Peak current at 0.36 V is proportional to Ag^+ concentration ranging from 0 nM to 400 nM. The fitting equation is $y=1.865x^2/(3284+x^2)$. The inset in Figure 5b shows the peak current is linearly dependent on Ag^+ concentration ranging from 10 nM to 150 nM. The fitting linear equation is $y=0.319+0.00967x$ ($R^2=0.982$). Limit of detection (LOD) for Ag^+ assay is found at 3.4 nM (about 0.37 ppb), which is estimated at the signal-to-noise ratio of 3. Obviously, SWV peak of MB shows similar dependence upon Hg^{2+} concentration (Figure 6). The fitting equation is $y=2.099x^2/(2910+x^2)$. The inset in Figure 6b shows the linear relationship between peak current and Hg^{2+} concentration ranging from 10 nM to 100 nM with the equation of $y=0.209+0.0163x$ ($R^2 = 0.985$). We have also calculated the LOD, which is as low as 1.7 nM (about 0.34 ppb). Both of the LODs for Ag^+ and Hg^{2+} could meet the needs of USEPA guidelines.[6-7] The analytical performances of this method is comparable or even better than most of recent reported methods for simultaneous detection (Table 1). The amplification-free feature of this method also makes it less time consuming compared with other sensitive methods which involve signal amplifications.[45-46] The precision of this method has been studied by measuring standard Ag^+ and Hg^{2+} solutions (10 nM, 50 nM, 100 nM) with identical batches of DNA modified magnetic NPs.

The measured values for each concentrations of target ions are close to each other and all relative standard deviations are within 8%. We have then prepared four batches of DNA modified magnetic NPs, which are used for the measurement of 400 nM Ag^{+} and Hg^{2+}, the signal intensities of SWV current peaks for MB and Fc are similar respectively and the relative standard deviations are within 5%. These results demonstrate satisfactory precision and reproducibility of this sensing strategy.

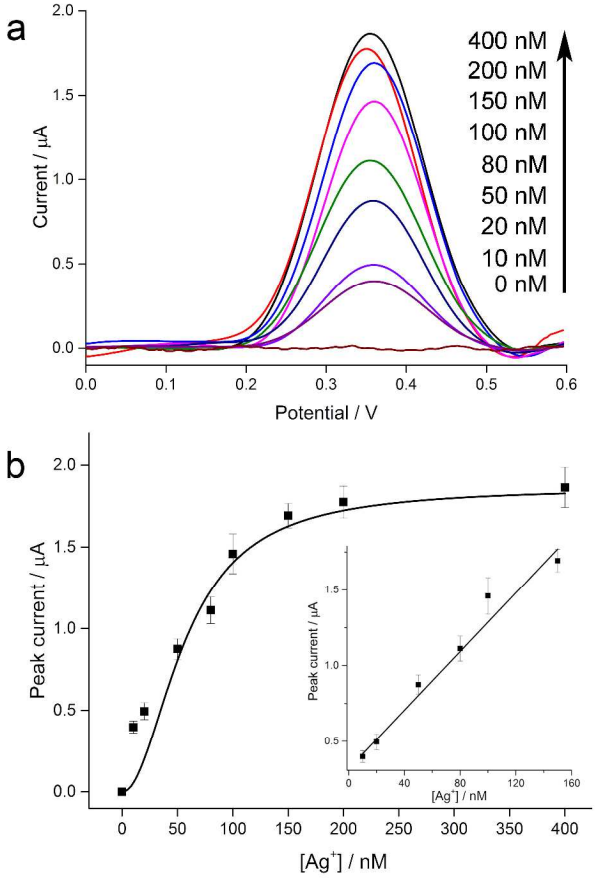

Figure 5. (a) SWVs for the detection of different concentrations of (a) Ag^{+} (from 0 nM to 400 nM). (b) Calibration curves of the analytical method for the detection of Ag^{+}. Inset shows the linear range. Error bars represented standard deviations of three independent measurements.

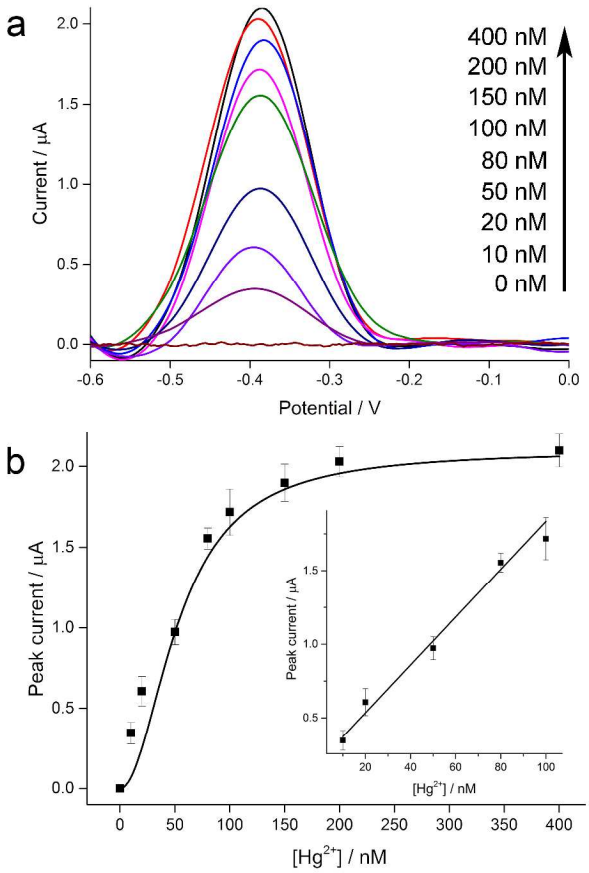

Figure 6. (a) SWVs for the detection of different concentrations of (a) Hg^{2+} (from 0 nM to 400 nM). (b) Calibration curves of the analytical method for the detection of Hg^{2+}. Inset shows the linear range. Error bars represented standard deviations of three independent measurements.

Table 1. Analytical performances of recent methods for simultaneous detection of heavy metal ions.

Methods	Detection range	LOD	Ref
Colorimetry	Ag^{+} (2 to 8 μM); Hg^{2+} (2 to 40 μM)	Ag^{+} (0.4 μM); Hg^{2+} (2 μM)	47
Colorimetry	Ag^{+} (0 to 200 μM); Hg^{2+} (0 to 200 μM)	Ag^{+} (1.69 μM); Hg^{2+} (0.19 μM)	29
fluorescence	Ag^{+} (0 to 1.75 μM); Hg^{2+} (0 to 3 μM)	Ag^{+} (47 nM); Hg^{2+} 121 nM)	48
fluorescence	Ag^{+} (6 to 650 nM); Hg^{2+} (5 to 1000 nM)	Ag^{+} (1.2 nM); Hg^{2+} (3.3 nM)	30
SERS	Ag^{+} (0.1 to 10000 nM); Hg^{2+} (1 to 10000 nM)	Ag^{+} (0.86 nM); Hg^{2+} (0.77 nM)	31
EIS	Ag^{+} (100 to 800 nM); Hg^{2+} (0.1 to 10000 nM)	Ag^{+} (10 nM); Hg^{2+} (0.1 nM)	49
SWV	Ag^{+} (10 to 150 nM); Hg^{2+} (10 to 100 nM)	Ag^{+} (3.4 nM); Hg^{2+} (1.7 nM)	this work

Selectivity Study. To evaluate the performance of a novel analytical method, selectivity is a critical index. Herein, a series of metal ions have been chosen and detected by the proposed method (Na^{+}, K^{+}, Pb^{2+}, Cd^{2+}, Zn^{2+}, Cu^{2+}, Ca^{2+}, Fe^{3+}, Cr^{3+}). The measurements are conducted by using 100 nM metal ions. As shown in Figure 7, Fc and MB current peaks which stand for Ag^{+} and Hg^{2+} levels are negligible in the absence of the corresponding target ions. The signals for Ag^{+} and Hg^{2+} are independent and no interference is observed. These results confirm the high

selectivity of the proposed method. We have also employed Ag^{+} (460 nM) and Hg^{2+} (10 nM) of toxicity levels defined by USEPA and compared the peak currents with the maximum values of interfering ions. Although the concentrations of these ions are relatively high, the generated peak currents are not significant and Ag^{+} or Hg^{2+} with critical values can be successfully distinguished.

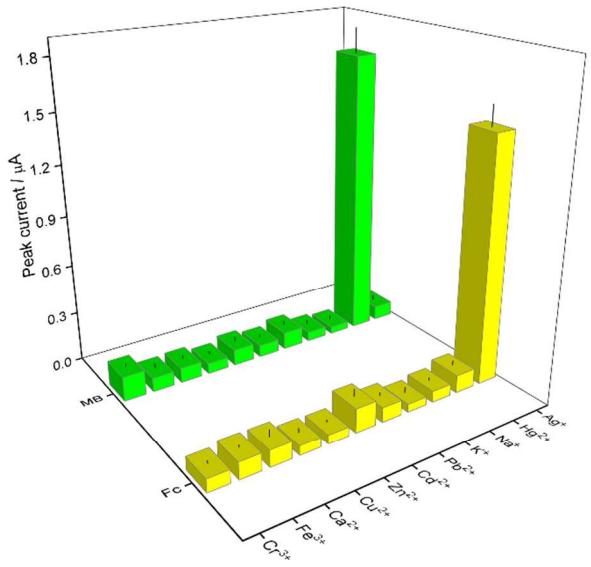

Figure 7. Selectivity of the analytical method for the detection of Ag^{+} and Hg^{2+}. The concentrations of the ions are 100 nM. Error bars represented standard deviations of three independent measurements.

Real Water Sample Analysis. To further evaluate the possible applications of the proposed sensing strategy in real samples, four water samples including Taihu Lake water, drinking water (Suzhou, China), orange juice and red wine are tested. Compared with standard mixture of Ag^{+}

and Hg^{2+} with relatively low concentrations of 10 nM, the current intensities at 0.36 V (Fc) and -0.39 V (MB) are quite weak, indicating that there are nearly no Ag^{+} and Hg^{2+} in the samples (Figure S4). We have then spiked different amount of Ag^{+} and Hg^{2+} into the four water samples. These prepared mixtures have been detected by the magnetic NPs based sensing method and atomic absorption spectroscopy (AAS), separately. The obtained results by the proposed method display satisfactory recoveries and acceptable accuracies, which also show fairly good concordance compared with AAS results (Table S2). Therefore, the method could be preliminarily utilized for the detection of heavy metal ions in real water samples.

CONCLUSIONS

In summary, we have prepared DNA modified magnetic NPs as selective electrochemical probes for simultaneous detection of Ag^{+} and Hg^{2+}. Of particular note, the modified Fe_3O_4@Au NPs can be firmly immobilized onto MGCE in just 2 min benefited from the magnetic property, eliminating complicated electrode modification process. Three DNA probes are modified with thiol groups and two electrochemical species (Fc and MB), respectively. Specific interactions of metal ions with mismatched base pairs (C-C and T-T) are designed in this sensing strategy. SWV signals for the Ag^{+} and Hg^{2+} are independent and simultaneous detection of the two heavy metal ions is achieved. Nanomolar sensitivities for the detection of the two heavy metal ions are obtained, which meet the requirements of USEPA. Moreover, by testing some common interfering metal ions, the negligible signals ensures the high selectivity of this multiplex analysis method towards target ions. The strategy is also successfully implemented in the analysis of Ag^{+} and Hg^{2+} in lake water, drinking water, orange juice, and red wine, which

exhibits fine utility for the monitoring of various real water samples. Aside from this, it is also simple, stable, cost-effective and amplification-free, which is well suitable for practical applications.

ASSOCIATED CONTENT

Supporting Information.

The Supporting Information is available free of charge on the ACS Publications website.

Additional figures and tables including photographs of MGCE, three electrode system and magnetic separation, optimization of magnetic NPs concentration and DNA 1 concentration, DNA sequences, results of multi-ion analysis in real water samples (PDF)

AUTHOR INFORMATION

Corresponding Author

* Tel.: +86-512-69588279. E-mail: miaopeng@sibet.ac.cn.

Notes

The authors declare no competing financial interest.

ACKNOWLEDGMENT

This work is supported by the National Natural Science Foundation of China (Grant No. 31400847).

REFERENCES

(1) Harrison, J. J.; Ceri, H.; Turner, R. J. Multimetal Resistance and Tolerance in Microbial Biofilms. *Nat. Rev. Microbiol.* **2007,** *5*, 928-938.

(2) Harada, M. Minamata Disease - Methylmercury Poisoning in Japan Caused by Environmental-Pollution. *Crit. Rev. Toxicol.* **1995,** *25*, 1-24.

(3) Torres, A. M.; Dnyanmote, A. V.; Bush, K. T.; Wu, W.; Nigam, S. K. Deletion of Multispecific Organic Anion Transporter Oat1/Slc22a6 Protects against Mercury-induced Kidney Injury. *J. Biol. Chem.* **2011,** *286*, 26391-26395.

(4) Wood, C. M.; Hogstrand, C.; Galvez, F.; Munger, R. S. The Physiology of Waterborne Silver Toxicity in Freshwater Rainbow Trout (Oncorhynchus Mykiss) .1. The Effects of Ionic Ag+. *Aquat. Toxicol.* **1996,** *35*, 93-109.

(5) Kumar, M.; Kumar, R.; Bhalla, V. Optical Chemosensor for Ag+, Fe3+, and Cysteine: Information Processing at Molecular Level. *Org. Lett.* **2011,** *13*, 366-369.

(6) EPA. *Ambient Water Quality Criteria for Silver*, Environmental Protection Agency, Office of Water, Washington, D.C. EPA 440/5-80-071, 1980.

(7) EPA. *Ambient Water Quality Criteria for Mercury*, U.S. Environmental Protection Agency, Office of Water, Washington, D.C. EPA 440/5-94-026, 1985.

(8) WHO. *Guidelines for Drinking-Water Quality, 4th ed*, WHO: Geneva, 2011.

(9) Zhou, X. J.; Nie, J. J.; Du, B. Y. 4-(2-Pyridylazo)-resorcinol Functionalized Thermosensitive Ionic Microgels for Optical Detection of Heavy Metal Ions at Nanomolar Level. *ACS Appl. Mater. Interfaces* **2015,** *7*, 21966-21974.

(10) Zang, J. C.; Li, C. G.; Zhou, K.; Dong, H. S.; Chen, B.; Wang, F. D.; Zhao, G. H. Nanomolar Hg2+ Detection Using beta-Lactoglobulin-Stabilized Fluorescent Gold Nanoclusters in Beverage and Biological Media. *Anal. Chem.* **2016,** *88*, 10275-10283.

(11) Mirzaei, M.; Behzadi, M.; Abadi, N. M.; Beizaei, A. Simultaneous Separation/Preconcentration of Ultra Trace Heavy Metals in Industrial Wastewaters by Dispersive Liquid-Liquid Microextraction Based on Solidification of Floating Organic Drop

Prior to Determination by Graphite Furnace Atomic Absorption Spectrometry. *J. Hazard. Mater.* **2011,** *186*, 1739-1743.

(12) Soto-Alvaredo, J.; Montes-Bayon, M.; Bettmer, J. Speciation of Silver Nanoparticles and Silver(I) by Reversed-Phase Liquid Chromatography Coupled to ICPMS. *Anal. Chem.* **2013,** *85*, 1316-1321.

(13) Cheng, G. H.; He, M.; Peng, H. Y.; Hu, B. Dithizone Modified Magnetic Nanoparticles for Fast and Selective Solid Phase Extraction of Trace Elements in Environmental and Biological Samples Prior to Their Determination by ICP-OES. *Talanta* **2012,** *88*, 507-515.

(14) Wang, H.; Wang, Y. X.; Jin, J. Y.; Yang, R. H. Gold Nanoparticle-Based Colorimetric and "Turn-On" Fluorescent Probe for Mercury(II) Ions in Aqueous Solution. *Anal. Chem.* **2008,** *80*, 9021-9028.

(15) Chen, Y. Y.; Chang, H. T.; Shiang, Y. C.; Hung, Y. L.; Chiang, C. K.; Huang, C. C. Colorimetric Assay for Lead Ions Based on the Leaching of Gold Nanoparticles. *Anal. Chem.* **2009,** *81*, 9433-9439.

(16) Miao, P.; Ning, L. M.; Li, X. X. Gold Nanoparticles and Cleavage-Based Dual Signal Amplification for Ultrasensitive Detection of Silver Ions. *Anal. Chem.* **2013,** *85*, 7966-7970.

(17) Nie, Z. H.; Nijhuis, C. A.; Gong, J. L.; Chen, X.; Kumachev, A.; Martinez, A. W.; Narovlyansky, M.; Whitesides, G. M. Electrochemical Sensing in Paper-Based Microfluidic Devices. *Lab Chip* **2010,** *10*, 477-483.

(18) Alvarez-Puebla, R. A.; Liz-Marzan, L. M. Environmental Applications of Plasmon Assisted Raman Scattering. *Energy Environ. Sci.* **2010,** *3*, 1011-1017.

(19) Ren, W.; Zhu, C. Z.; Wang, E. K. Enhanced Sensitivity of a Direct SERS Technique for Hg2+ Detection Based on the Investigation of the Interaction Between Silver Nanoparticles and Mercury Ions. *Nanoscale* **2012,** *4*, 5902-5909.

(20) Neupane, L. N.; Oh, E. T.; Park, H. J.; Lee, K. H. Selective and Sensitive Detection of Heavy Metal Ions in 100% Aqueous Solution and Cells with a Fluorescence Chemosensor Based on Peptide Using Aggregation-Induced Emission. *Anal. Chem.* **2016,** *88*, 3333-3340.

(21) Wang, Z. X.; Ding, S. N. One-Pot Green Synthesis of High Quantum Yield Oxygen-Doped, Nitrogen-Rich, Photoluminescent Polymer Carbon Nanoribbons as an Effective Fluorescent Sensing Platform for Sensitive and Selective Detection of Silver(I) and Mercury(II) Ions. *Anal. Chem.* **2014,** *86*, 7436-7445.

(22) Khani, H.; Rofouei, M. K.; Arab, P.; Gupta, V. K.; Vafaei, Z. Multi-Walled Carbon Nanotubes-Ionic Liquid-Carbon Paste Electrode as a Super Selectivity Sensor: Application to Potentiometric Monitoring of Mercury Ion(II). *J. Hazard. Mater.* **2010,** *183*, 402-409.

(23) Zhang, Y.; Zeng, G. M.; Tang, L.; Chen, J.; Zhu, Y.; He, X. X.; He, Y. Electrochemical Sensor Based on Electrodeposited Graphene-Au Modified Electrode and NanoAu Carrier Amplified Signal Strategy for Attomolar Mercury Detection. *Anal. Chem.* **2015,** *87*, 989-996.

(24) Childress, E. S.; Roberts, C. A.; Sherwood, D. Y.; LeGuyader, C. L. M.; Harbron, E. J. Ratiometric Fluorescence Detection of Mercury Ions in Water by Conjugated Polymer Nanoparticles. *Anal. Chem.* **2012,** *84*, 1235-1239.

(25) Darbha, G. K.; Singh, A. K.; Rai, U. S.; Yu, E.; Yu, H. T.; Ray, P. C. Selective Detection of Mercury (II) Ion Using Nonlinear Optical Properties of Gold Nanoparticles. *J. Am. Chem. Soc.* **2008,** *130*, 8038-8043.

(26) Yang, Y.; Liu, T.; Cheng, L.; Song, G. S.; Liu, Z.; Chen, M. W. MoS2-Based Nanoprobes for Detection of Silver Ions in Aqueous Solutions and Bacteria. *ACS Appl. Mater. Interfaces* **2015,** *7*, 7526-7533.

(27) Lu, M. H.; Xiao, R.; Zhang, X. N.; Niu, J. H.; Zhang, X. T.; Wang, Y. M. Novel Electrochemical Sensing Platform for Quantitative Monitoring of Hg(II) on DNA-Assembled Graphene Oxide with Target Recycling. *Biosens. Bioelectron.* **2016,** *85*, 267-271.

(28) Chu, K. W.; Chow, K. L. Synergistic Toxicity of Multiple Heavy Metals is Revealed by a Biological Assay Using a Nematode and Its Transgenic Derivative. *Aquat. Toxicol.* **2002,** *61*, 53-64.

(29) Liu, L.; Lin, H. W. Paper-Based Colorimetric Array Test Strip for Selective and Semiquantitative Multi-Ion Analysis: Simultaneous Detection of Hg2+, Ag+, and Cu2+. *Anal. Chem.* **2014,** *86*, 8829-8834.

(30) Zuo, X. W.; Zhang, H. G.; Zhu, Q.; Wang, W. F.; Feng, J.; Chen, X. G. A Dual-Color Fluorescent Biosensing Platform Based on WS2 Nanosheet for Detection of Hg2+ and Ag+. *Biosens. Bioelectron.* **2016,** *85*, 464-470.

(31) Zeng, Y.; Ren, J. Q.; Shen, A. G.; Hu, J. M. Field and Pretreatment-Free Detection of Heavy-Metal Ions in Organic Polluted Water through an Alkyne-Coded SERS Test Kit. *ACS Appl. Mater. Interfaces* **2016,** *8*, 27772-27778.

(32) Su, S.; Wu, Y.; Zhu, D.; Chao, J.; Liu, X. F.; Wan, Y.; Su, Y.; Zuo, X. L.; Fan, C. H.; Wang, L. H. On-Electrode Synthesis of Shape-Controlled Hierarchical Flower-Like Gold Nanostructures for Efficient Interfacial DNA Assembly and Sensitive Electrochemical Sensing of MicroRNA. *Small* **2016,** *12*, 3794-3801.

(33) Yang, G. H.; Zhu, C. Z.; Du, D.; Zhu, J. J.; Lin, Y. H. Graphene-Like Two-Dimensional Layered Nanomaterials: Applications in Biosensors and Nanomedicine. *Nanoscale* **2015,** *7*, 14217-14231.

(34) Dong, S. B.; Zhao, R. T.; Zhu, J. G.; Lu, X.; Li, Y.; Qiu, S. F.; Jia, L. L.; Jiao, X.; Song, S. P.; Fan, C. H.; Hao, R. Z.; Song, H. B. Electrochemical DNA Biosensor Based on a Tetrahedral Nanostructure Probe for the Detection of Avian Influenza A (H7N9) Virus. *ACS Appl. Mater. Interfaces* **2015,** *7*, 8834-8842.

(35) Deng, Y. Y.; Li, E. D.; Cheng, X. J.; Zhu, J.; Lu, S. L.; Ge, C. C.; Gu, H. W.; Pan, Y. Facile Preparation of Hybrid Core-Shell Nanorods for Photothermal and Radiation Combined Therapy. *Nanoscale* **2016,** *8*, 3895-3899.

(36) Zhu, J.; Lu, Y. J.; Li, Y. G.; Jiang, J.; Cheng, L.; Liu, Z.; Guo, L.; Pan, Y.; Gu, H. W. Synthesis of Au–Fe3O4 Heterostructured Nanoparticles for In Vivo Computed Tomography and Magnetic Resonance Dual Model Imaging. *Nanoscale* **2014,** *6*, 199-202.

(37) Freitas, M.; Couto, M. S.; Barroso, M. F.; Pereira, C.; de-los-Santos-Alvarez, N.; Miranda-Ordieres, A. J.; Lobo-Castanon, M. J.; Delerue-Matos, C. Highly Monodisperse Fe3O4@Au Superparamagnetic Nanoparticles as Reproducible Platform for Genosensing Genetically Modified Organisms. *ACS Sens.* **2016,** *1*, 1044-1053.

(38) Narayanan, S.; Sathy, B. N.; Mony, U.; Koyakutty, M.; Nair, S. V.; Menon, D. Biocompatible Magnetite/Gold Nanohybrid Contrast Agents via Green Chemistry for MRI and CT Bioimaging. *ACS Appl. Mater. Interfaces* **2012,** *4*, 251-260.

(39) Wu, L. H.; Mendoza-Garcia, A.; Li, Q.; Sun, S. H. Organic Phase Syntheses of Magnetic Nanoparticles and Their Applications. *Chem. Rev.* **2016,** *116*, 10473-10512.

(40) Rao, L.; Bu, L. L.; Xu, J. H.; Cai, B.; Yu, G. T.; Yu, X. L.; He, Z. B.; Huang, Q. Q.; Li, A.; Guo, S. S.; Zhang, W. F.; Liu, W.; Sun, Z. J.; Wang, H.; Wang, T. H.; Zhao, X. Z. Red Blood Cell Membrane as a Biomimetic Nanocoating for Prolonged Circulation Time and Reduced Accelerated Blood Clearance. *Small* **2015,** *11*, 6225-6236.

(41) Miao, P.; Wang, B. D.; Yu, Z. Q.; Zhao, J.; Tang, Y. G. Ultrasensitive Electrochemical Detection of microRNA with Star Trigon Structure and Endonuclease Mediated Signal Amplification. *Biosens. Bioelectron.* **2015,** *63*, 365-370.

(42) Ono, A.; Cao, S.; Togashi, H.; Tashiro, M.; Fujimoto, T.; Machinami, T.; Oda, S.; Miyake, Y.; Okamoto, I.; Tanaka, Y. Specific Interactions between Silver(I) Ions and Cytosine-Cytosine Pairs in DNA Duplexes. *Chem. Commun.* **2008**, 4825-4827.

(43) Ono, A.; Togashi, H. Highly Selective Oligonucleotide-Based Sensor for Mercury(II) in Aqueous Solutions. *Angew. Chem., Int. Ed.* **2004,** *43*, 4300-4302.

(44) Wu, C. S.; Oo, M. K. K.; Fan, X. D. Highly Sensitive Multiplexed Heavy Metal Detection Using Quantum-Dot-Labeled DNAzymes. *ACS Nano* **2010,** *4*, 5897-5904.

(45) Miao, P.; Han, K.; Wang, B. D.; Luo, G. Y.; Wang, P.; Chen, M. L.; Tang, Y. G. Electrochemical Detection of Aqueous Ag+ Based on Ag+ -Assisted Ligation Reaction. *Sci Rep* **2015,** *5*, 9161.

(46) Zhu, Z. Q.; Su, Y. Y.; Li, J.; Li, D.; Zhang, J.; Song, S. P.; Zhao, Y.; Li, G. X.; Fan, C. H. Highly Sensitive Electrochemical Sensor for Mercury(II) Ions by Using a Mercury-Specific Oligonucleotide Probe and Gold Nanoparticle-Based Amplification. *Anal. Chem.* **2009,** *81*, 7660-7666.

(47) Zhang, Y. H.; Liu, W.; Zhang, W. T.; Yu, S. X.; Yue, X. Y.; Zhu, W. X.; Zhang, D. H.; Wang, Y. R.; Wang, J. L. DNA-Mediated Gold Nanoparticle Signal Transducers for

Combinatorial Logic Operations and Heavy Metal Ions Sensing. *Biosens. Bioelectron.* **2015,** *72*, 218-224.

(48) Zhang, Y. L.; Zuo, P.; Ye, B. C. A Low-Cost and Simple Paper-Based Microfluidic Device for Simultaneous Multiplex Determination of Different Types of Chemical Contaminants in Food. *Biosens. Bioelectron.* **2015,** *68*, 14-19.

(49) Lin, Z. Z.; Li, X. H.; Kraatz, H. B. Impedimetric Immobilized DNA-Based Sensor for Simultaneous Detection of Pb2+, Ag+, and Hg2+. *Anal. Chem.* **2011,** *83*, 6896-6901.

For Table of Contents Only